Physics in Medicine & Biology

Walled vessel-mimicking phantom for ultrasound imaging using 3D printing with a water-soluble filament: design principle, fluid-structure interaction (FSI) simulation, and experimental validation

To cite this article before publication: Jinping Dong *et al* 2020 *Phys. Med. Biol.* in press https://doi.org/10.1088/1361-6560/ab7abf

Walled vessel-mimicking phantom for ultrasound imaging using 3D printing with a water-soluble filament: design principle, fluid-structure interaction (FSI) simulation, and experimental validation

Jinping Dong[1], Yang Zhang[1] and Wei-Ning Lee[1,2]

1. Department of Electrical and Electronic Engineering, The University of Hong Kong, Hong Kong
2. Biomedical Engineering Programme, The University of Hong Kong, Hong Kong

Email: wnlee@eee.hku.hk

Keywords: artery, blood flow, elasticity, polyvinyl alcohol (PVA), ultrasound

Abstract

The geometry and stiffness of a vessel are pertinent to blood dynamics and vessel wall mechanical behavior and may alter in diseased conditions. Ultrasound-based ultrafast Doppler (uDoppler) imaging and shear wave imaging (SWI) techniques have been extensively exploited for the assessment of vascular hemodynamics and mechanics. Their performance is conventionally validated on vessel-mimicking phantoms (VMPs) prior to their clinical use. Compared with commercial ones, customized VMPs are favored for research use because of their wider range of material properties, more complex lumen geometries, or wall structures. Fused deposition modeling (FDM) 3D printing technique with plastic filaments is a promising method for making VMPs with a complex vessel lumen. However, it may require a toxic solvent or a long dissolution time currently. In this paper, we present a safe, efficient and geometrically flexible method where FDM 3D printing with a water-soluble polyvinyl alcohol (PVA) filament is exploited to fabricate a walled three-branch VMP (VMP-I). As a key step in fabrication, to avoid dissolution of the PVA-printed vessel core by the solution of the tissue-mimicking material, paraffin wax was used for isolation. Paraffin wax is easy to coat (i.e., without any special equipment), of satisfactory thickness (~0.1 mm), chemically stable, easy to remove after fabrication, thus making the proposed method practicable for ultrasound imaging studies. VMP-I was examined by B-mode imaging and power Doppler imaging (PDI) to verify complete dissolution of PVA-printed vessel core in its lumen, confirming good fabrication quality. The flow velocities in VMP-I were estimated by uDoppler imaging with a -0.8% difference, and the shear wave propagation speeds for the same phantom were estimated by SWI with a -6.03% difference when compared with fluid-structure interaction (FSI) simulation results. A wall-less VMP of a scaled and simplified coronary arterial network (VMP-II) was additionally fabricated and examined to test the capability of the proposed method for a complex lumen geometry. The proposed fabrication method for customized VMPs is foreseen to facilitate the development of ultrasound imaging techniques for blood vessels.

1 Introduction

Cardiovascular diseases (CVDs) cause the highest mortality globally according to the World Health Organization (WHO, 2017). The high temporal resolution, noninvasiveness, safety, portability and cost-effectiveness of ultrasound imaging collectively render it the predominant medical imaging modality for diagnosis of CVDs. In particular, ultrasound imaging techniques that assess vascular function are indispensable to detect the onset of diseases attributed to vascular impairment.

Many ultrasound imaging techniques have been developed to evaluate vascular function by visualizing and quantifying blood dynamics inside the lumen or mechanics of the vessel wall. Power

Doppler imaging (PDI) (Hudson-Dixon *et al.*, 1999), color Doppler imaging (CDI) (Evans *et al.*, 2011), and ultrafast Doppler (uDoppler) imaging (Bercoff *et al.*, 2011) use the Doppler effect to map blood perfusion and detect abnormal fluid dynamics. For example, as a uDoppler imaging method, vector projectile imaging was demonstrated to be a potential tool for complex flow analysis in blood vessel (Yiu *et al.*, 2014). Separately, ultrasound-based shear wave imaging (SWI) (Couade *et al.*, 2010) and pulse wave imaging (PWI) (Vappou *et al.*, 2010) have been demonstrated to be capable of noninvasively estimating the stiffness of the blood vessel wall, which alters in impaired cardiovascular conditions. Recently, SWI was further developed to estimate both the longitudinal and transverse stiffnesses of the artery (He *et al.*, 2017; Guo *et al.*, 2017; Guo *et al.*, 2018) under various luminal pressures (Wang *et al.*, 2019), thus enabling comprehensive characterization of the arterial wall.

Vessel-mimicking phantoms (VMPs) are essential to validate ultrasound imaging techniques for the blood vessel before their clinical use. One study used a VMP with two layers of different stiffnesses to evaluate the performance of noninvasive high-frequency vascular ultrasound elastography in estimating the 2D-strain tensor of superficial arteries (Maurice *et al.*, 2005). In another study, polyacrylamide-based straight-geometry VMPs were used to validate ultrasound PWI with the Moens-Korteweg equation for wall stiffness estimation (Shahmirzadi *et al.*, 2012). All aforementioned studies demonstrated the importance of VMPs for development of vascular ultrasound imaging techniques.

Although several commercial VMPs are available for clinical training (Cournane *et al.*, 2012; Luyet *et al.*, 2011) or academic research, their relatively simple lumen geometries limit their applications in quantification of blood dynamics. A lack of vessel wall structures in some commercial VMPs hinders them from evaluation of ultrasound elasticity imaging methods for the vessel wall. Favored for ultrasound imaging studies, high quality fabrication of customized VMPs should include several features as follows:

- It should be geometrically flexible enough to fabricate different vessel lumens.
- The vessel wall structure with a surrounding medium is a requisite in VMPs when estimating mechanical properties of the vessel wall.
- Acoustic and mechanical properties of all the structures in VMPs should be close to the real ones to better mimic vascular behavior. For example, soft-tissue-mimicking materials, instead of water, are preferred to be serve as a surrounding medium.
- It is safer when no toxic chemicals are included in the entire fabrication procedure.
- The fabrication process should be efficient and straightforward;
- The results obtained from ultrasound imaging of VMPs can be compared with a fluid-structure interaction (FSI) simulation, which provides numerical results of blood dynamics and wall mechanical behavior. It is thus helpful to establish an FSI model that works together with VMPs as an integrated tool for development of ultrasound imaging techniques.

Tremendous efforts have been made for identifying suitable soft-tissue-mimicking materials. Reported materials for ultrasound tissue-mimicking phantoms (TMPs) include agar/gelatin (Pavan *et al.*, 2010), PVA-H (polyvinyl alcohol hydrogel) (Surry *et al.*, 2004; Xia *et al.*, 2011), silicone (McLeod *et al.*, 2016), polyvinyl chloride-plastisol (McLeod *et al.*, 2015), urethane rubber (Culjat *et al.*, 2010), oil-based materials (Maneas *et al.*, 2018) and so on. Among them, agar/gelatin and PVA-H are commonly used because their acoustic (e.g., speed of sound, acoustic impedance, attenuation) and mechanical properties (e.g., density, compressibility, stiffness, viscosity,

nonlinearity) are close to those of real soft tissues (White *et al.*, 1998). Stiffness of the TMPs increases with gelatin concentration, allowing one to make an inhomogeneous agar/gelatin phantom. For example, a harder cylindrical inclusion made of 1%/8% agar/gelatin with 20 mm in diameter was embedded in a 1%/5% agar/gelatin mixture to evaluate the performance of supersonic shear imaging (SSI) (Bercoff *et al.*, 2004). Similarly, a higher concentration of PVA-H or a larger number of freeze/thaw (F/T) cycles produces a stiffer PVA-H phantom. As measured by mechanical testing, the average Young's modulus of 10% PVA-H TMPs was 42.8kPa for two F/T cycles and 89.1kPa for five F/T cycles (Fromageau *et al.*, 2003), which are in the range of commonly known soft tissue stiffness. PVA-H was further reported to be able to make a transversely isotropic TMP by keeping it stretched during F/T cycles for fibrous soft tissues (Chatelin *et al.*, 2014), e.g., cardiovascular tissue (Millon *et al.*, 2006). PVA-H additionally enjoys good mechanical strength and long preservation, making it a useful tissue-mimicking material for ultrasound imaging as well as other imaging modalities, such as magnetic resonance imaging (MRI) (Surry *et al.*, 2004) and photoacoustic imaging (Xia *et al.*, 2011). For blood-mimicking fluid (BMF), a standard protocol was established to fabricate BMF with its density, viscosity and other acoustic and mechanical properties similar to those of human blood (Ramnarine *et al.*, 1998), and it was widely adopted in ultrasound-based blood flow imaging studies *in vitro* (Ho *et al.*, 2017; Wei *et al.*, 2018; Yiu *et al.*, 2019).

Various approaches have been proposed to make VMPs with rather complex geometry. A wall-less VMP could be made using computerized milling with a rigid material (Wong *et al.*, 2008). Rapid prototyping with a compliant photopolymer filament (Lai *et al.*, 2013) enabled direct fabrication of complex vessel lumen geometries and made three walled carotid bifurcation VMPs with 50% eccentric stenosis and plaque ulcerations. The stiffness of the fabricated VMPs (391 kPa Young's modulus) was in the normal range, but their acoustic properties (1801 m/s speed of sound, $1.58\ \mathrm{dB/(mm \cdot MHz^{0.97})}$ attenuation coefficient) were higher than those of real human arteries (Ryan and Foster, 1997). In a later study, a negative mold was first made by rapid prototyping, and a wall-less carotid bifurcation phantom was fabricated by injecting melted wax into the mold to cast the vessel core. The wax was finally fractured after PVA-H underwent 3 F/T cycles, and the final VMP was shown feasible to evaluate color-encoded speckle imaging (Yiu and Alfred, 2013) and vector projectile imaging (Yiu *et al.*, 2014). Recently, fused deposition modeling (FDM) 3D printing with a polylactic acid (PLA) filament was utilized to print the vessel core and the casting mold. After assembling the vessel core and the casting mold, the PVA-H solution was injected and underwent 3 F/T cycles. The core was then removed after being cracked gently, and the vessel wall was lastly embedded in an agar/gelatin bulk for further testing. The proposed method was demonstrated to be feasible to make walled carotid phantom for ultrasound flow imaging with vessel wall motion (Chee *et al.*, 2016). Later, a similar method was adopted to manufacture a patient-specific wall-less VMP based on CT images and verified by ultrasound flow imaging. Nevertheless, the vessel core printed by the PLA filament had to be dissolved by Chloroform (Ho *et al.*, 2017), which was toxic and required long dissolution time despite the flexibility of the proposed 3D printing technique and good printing quality of the PLA filament. Recently, the method that used FDM 3D printing with a water-soluble PVA filament was developed to fabricate VMP ((Mackle *et al.*, 2019)). It used Parylene to isolate the PVA-printed vessel core and the gel solution, but the requirement of special coating equipment limited its widespread use.

The goal of this study is to develop a tool that integrates VMP fabrication and fluid-structure interaction (FSI) simulation for experimental performance evaluation of vascular ultrasound imaging techniques. The study objectives are thus twofold. One is to develop a safe, efficient and geometrically flexible method that utilizes an FDM 3D printing technique and a water-soluble PVA filament to fabricate VMPs without the need of a toxic solvent or long dissolution time. In particular, the use of paraffin wax for isolation in our proposed method makes the fabrication more practicable because no special coating equipment is required. The other is to quantify blood flow velocities and vessel wall stiffness of VMPs using uDoppler imaging and SWI and compare them with FSI simulation predictions.

2 Methods

2.1 VMP fabricating procedure

Three key steps of the proposed VMP fabrication method are summarized in figure 1.

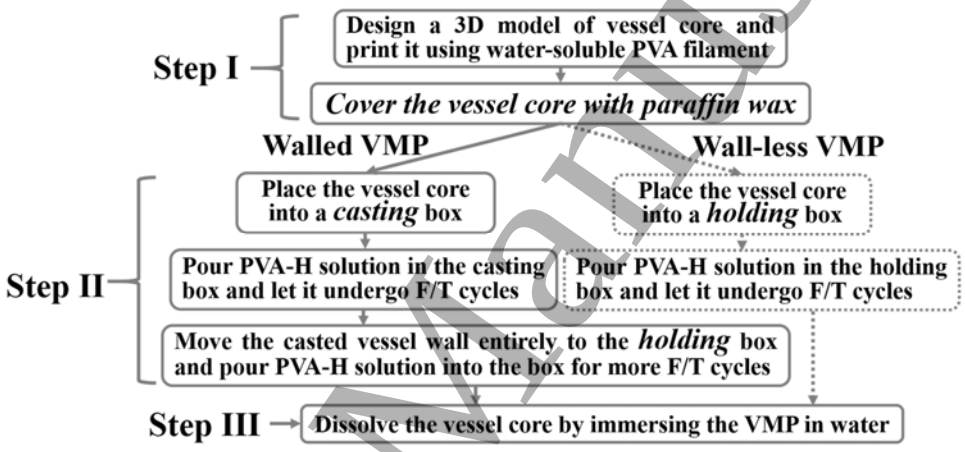

Figure 1. Key steps of the proposed vessel-mimicking phantom (VMP) fabrication method (Step I is the vessel core preparation; Step II is the VMP fabrication; and Step III is the vessel core dissolution). PVA: polyvinyl alcohol; PVA-H: polyvinyl alcohol hydrogel; F/T cycle: freeze/thaw cycle.

2.1.1 Design and printing of the 3D model of vessel core

A walled, three-branch VMP (VMP-I) was made to test the quality of wall structure by the proposed method. First, one 3D geometrical model of the vessel core for VMP-I was designed using Solidworks2016 software (Dassault Systemes, Waltham, MA, USA). The major vessel structure (figures 2(a) ③) with 4 mm in diameter was designed for VMP-I. A casting compartment with the vessel core geometry of VMP-I with a diameter of 8 mm was designed to fabricate a vessel wall structure with 2 mm thickness for VMP-I (figure 2(b)). A 121 mm×76 mm×76 mm (length×width×height) holding box with 3 mm wall thickness was designed and printed to hold the vessel core when filling the surrounding medium for VMP-I. Standard Tessellation Language (STL) files that contained structural information of the virtual 3D model as a meshwork of triangular surfaces were saved in Solidworks2016 for further 3D printing.

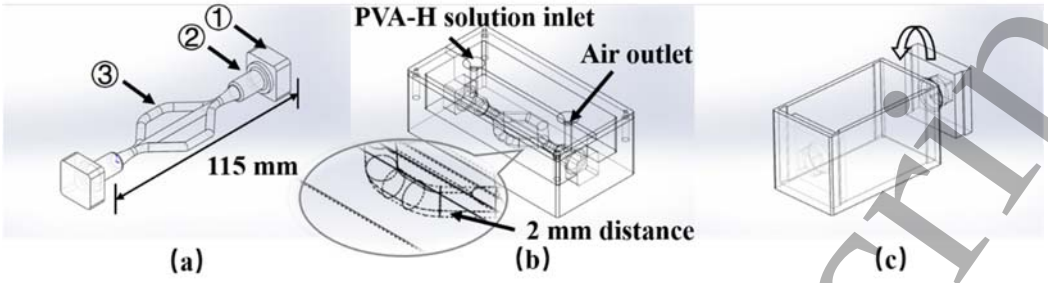

Figure 2. (a) 3D model of the vessel core for vessel-mimicking phantom I (VMP I). ① the holding part, ② the connecting part and ③ the major vessel structure (4 mm in diameter); **(b) The casting box for vessel wall fabrication in VMP I**; **(c) The holding box for VMP I**. Note that all the 3D models were designed using Solidworks2016.

An FDM 3D printer (CreatBot DX plus, Zhengzhou, China) with two extruders of 0.4 mm nozzle diameters was used in this study (figure 3(a), left). Its building volume is 300 mm×250 mm×520 mm with a spatial resolution of 0.02 mm along the height direction and 0.05 mm along the other two directions, enabling it to print a relatively large structure with good printing quality using PLA or ABS (Acrylonitrile Butadiene Styrene) filaments. The default slicing software (CreatWare V6.4.6) of the 3D printer was used to slice all the STL files using the printing parameters in Table 1. Since the water-soluble PVA filament may become too soft to print in a humid environment, it is necessary to control the humidity, especially for the 3D printer deployed herein that feeds the filament remotely. Consequently, a dehumidifier (Fortress FDH1816) was used in an enclosed room to control the humidity to stay below 40%, and meanwhile, a filament dryer (PrintDry, Windsor, Canada) (figure 3(a), right) was used at 45℃ to keep the water-soluble PVA filament dry when printing the vessel core. The printing quality was guaranteed by setting 220℃ extruder temperature, 20 mm/s printing speed and 75% global speed to ensure the water-soluble PVA filament to fuse completely while printing (Table 1). Note that these printing parameters were optimized and summarized after systematic trials. Moreover, high-temperature double-sided tapes were used to adhere the printing models to the heating bed of the 3D printer. Except the vessel core (figures 3(b)), which was printed by the water-soluble PVA filament, the other structures were all printed using the PLA filament.

As summarized in figure 1, a wall-less VMP can also be fabricated by following the same steps of the proposed method without casting the wall structure. Since it is difficult to design a casting box for a lumen with a complex 3D geometry, such as the coronary artery, a wall-less type is deemed more appropriate. For illustration, a wall-less VMP, whose geometry referenced to a simplified coronary artery model scaled by 0.5 (VMP-II), was also made. Its B-mode image and power Doppler image are shown and presented in the Discussion section.

Table 1 Printing parameters

Key parameters	Filament type	
	PVA	PLA
Extruder number	#1	#2
Extruder temperature	220℃	210℃
Bed temperature	65℃	45℃
Printing speed	20 mm/s	45 mm/s
Fill density	30%-40%	30%
Supporting density	25%	25%
Platform adhesion type	Raft	Raft
Retraction speed	30 mm/s	30 mm/s
Retraction distance	6 mm	6 mm
Global speed	75%	100%
Filament dryer temperature	45℃	N/A

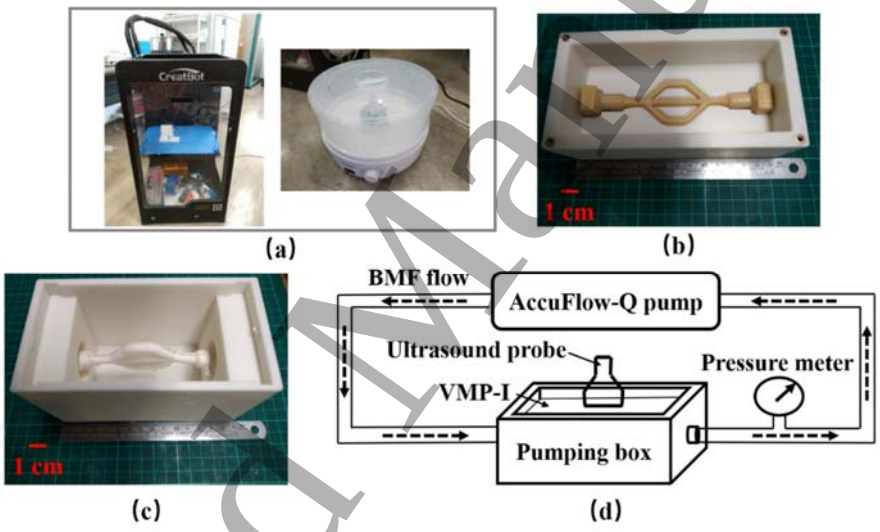

Figure 3. (a) A CreatBot DX plus 3D printer (left) and a PrintDry filament dryer (right); **(b) The vessel core of the vessel-mimicking phantom I (VMP-I, water-soluble PVA) in its casting box (PLA) before casting the vessel wall**; **(c) The vessel core of VMP-I with its casted vessel wall in the holding box (PLA)**. Note that all the models in (b) and (c) were printed by CreatBot DX plus; **(d) A schematic of the experimental setup for testing VMP-I**. BMF: blood-mimicking fluid.

2.1.2 Vessel-mimicking phantom (VMP) fabrication

Because the vessel core of VMP-I, which was printed with the water-soluble PVA filament, might be dissolved by the PVA-H solution, it was coated with a layer of paraffin wax for insulation. One-kg paraffin wax (melting point 56℃) was first put into a 4-liter glass beaker and heated up to 90℃ for 3 hours until it was melted completely. The vessel core was then dipped into the melted paraffin wax shortly for coating a thin layer of paraffin wax. Note that it might lead to some irregular (or uneven) surfaces in the vessel lumens or a failure of the final VMP fabrication due to partial dissolution of lumen core in the case of incomplete coverage of paraffin wax. After that, the vessel core of VMP-I was placed in its casting box to fabricate the vessel wall structure (figure 3(b)). Note

that the casting box had previously stored in a -20°C freezer for 3 hours before it was filled with PVA-H solutions to accelerate solidification for homogeneity of the final VMP.

Two batches of PVA-H solutions with different amounts of scatterers were prepared for the vessel wall structure and the surrounding medium, respectively. For the vessel wall structure, the PVA-H powder (10% by weight, 341584, Sigma-Aldrich) was added into a beaker of 50 ml deionized (DI) water (Millipore, Milli-DI systems, DI-PAK (Large)) on an electromagnetic stirrer. After covered by tinfoil to avoid losing DI water from evaporation, the beaker containing PVA-H mixture was moved into a water bath that was continuously heated at 90°C on an electromagnetic oven for 3 hours. As soon as the PVA-H powder was dissolved completely, the beaker was moved back to the electromagnetic stirrer to cool down while being stirred. SiO_2 powder (3% by weight, S5631, Sigma-Aldrich) as ultrasonic scatterers and potassium sorbate (1% by weight, 85520, Sigma-Aldrich) as an antibacterial agent were later added into the beaker at 50°C. The PVA-H solution was then continually cooled down for 30 minutes in an iced water bath.

Separately, 10% PVA-H powders, 1% SiO_2, 1% potassium sorbate, and 800 ml DI water were used and followed the aforementioned procedure to prepare PVA-H solution for the surrounding medium.

After preparing the PVA-H solutions, the one with 3% SiO_2 was poured into the casting box through its inlet (figure 2(b)) for VMP-I, and underwent 2 F/T cycles (12 hours/12 hours, -20°C/20°C) to cross-link the PVA-H. The congealed hydrogel phantom was moved entirely from the casting box to the holding box (figure 3(c)); the PVA-H solution with 1% SiO_2 was poured into the holding box for three more F/T cycles to fabricate the surrounding medium. Note that the number of F/T cycles was determined according to the mechanical and acoustic properties of the final VMP as suggested in literature (Hoskins, 2007; Fromageau *et al.*, 2007). Despite both being made of 10% PVA-H, the vessel wall structure had 3% SiO_2 and underwent 5 F/T cycles, while the surrounding medium had 1% SiO_2 and underwent 3 F/T cycles. VMP-I would exhibit brightness and stiffness contrasts between its vessel wall and surrounding medium due to the different amounts of SiO_2 and the different numbers of F/T cycles, making it useful to verify both ultrasound flow imaging and ultrasound elastography.

Finally, VMP-I was unmounted from its holding box, immersed in water for 3 hours to dissolve the PVA-printed vessel core. To remove the paraffin wax and the remains of its vessel core, VMP-I was massaged to fracture the paraffin wax before moving to the pumping box, and flushed using a small gear pump for five minutes.

A BMF, instead of distilled water, was used to better mimic the flow behavior of real human blood. The BMF was made of 83.7% (by weight) DI water, 0.3% potassium sorbate (85520, Sigma-Aldrich) as the antibacterial agent, 3.3% dextran (D4876, Sigma-Aldrich) to tune the viscosity, 10.0% glycerol (15514-029, Thermo Fisher Scientific, Waltham, MA, USA) to adjust the acoustic speed and density, 0.9% Tergitol surfactants (86453, Sigma-Aldrich), and 1.8% Orgasol (2001 UD NAT1, Arkema, Paris, France) to serve as acoustic scatterers of 5 μm diameter (Ramnarine *et al.*, 1998).

2.2 Vessel-mimicking Phantom (VMP) validation

2.2.1 Experimental setup and testing procedure

After fabricating VMP-I, a SONIX RP ultrasound system (Ultrasonix Medical Corporation, Richmond, BC, Canada) with a linear array probe L14-5/38 (bandwidth: 14–5MHz; Analogic Ultrasound, Richmond, BC, Canada) was first utilized to visualize its interior on B-mode and to confirm the complete dissolution of the PVA-printed vessel core using PDI. As shown in figure 3(d),

a VMP in its pumping box was connected to a flow pump (AccuFlow-Q; Shelley Medical Imaging, London, ON, Canada), which permitted controllable flow rates (0.01 to 35 ml/s) and flow types. The BMF was driven to flow inside the lumen of VMP-I by the flow pump with a constant flow of 2 ml/s in all tests. Additionally, an absorbing rubber layer was placed at the bottom of the pumping box to minimize acoustic reflections.

For B-mode imaging, 'general mode' with center frequency of 10 MHz and a depth of 9 cm were set. The inner diameter and the wall thickness of VMP-I were measured manually on the B-mode images using the built-in 'measurement' function to compare with the ground truth in 3D geometrical model. For PDI, 'power Doppler mode' with a pulse repetition frequency (PRF) of 1 kHz and a wall filter with a cut off frequency of 100 Hz was activated. PDI displays the amplitude of the Doppler signal and is sensitive to detect small blood vessels and relatively slow-moving blood (Hudson-Dixon *et al.*, 1999). It hereby helped us to check the fabrication quality of VMP-I from the aspect of flow conditions.

To further evaluate its performance in blood dynamics and mechanical property estimation on vessel wall, VMP-I was tested by uDoppler imaging and SWI, respectively, using a Vantage 256 system (Verasonics Inc., Kirkland, WA) with the same experimental setup as shown in figure 3(d). For uDoppler imaging, the Vantage system and an L11-4v probe (128 elements, Verasonics Inc., Kirkland, WA) operating at the center frequency of 6.25 MHz were used to realize ultrafast image sequences based on coherent plane wave compounding (CPWC) with three steered plane waves (-10°, 0°, 10°) at the compounded rate of 3000 frames per second (fps) (Tanter and Fink, 2014). A singular value decomposition (SVD) filter of 60 frames was used for clutter filtering (Demené *et al.*, 2015), and the axial and lateral motions of the flow were obtained by the spatial angular compounding method (Yiu *et al.*, 2014).

The same Vantage system and an L7–4 probe (128 elements, Verasonics Inc., Kirkland, WA) were used for SWI. Shear waves were remotely induced on the walls of the three branches of VMP-I by 100-μs ultrasonic focused beams with a center frequency of 5 MHz. The foci were set at three different depths of 33 mm, 43.5mm, 54 mm (F-number =0.86, 1.14, 1.41) to cover all the three branches of VMP-I in one sitting. Note that shear waves became guided due to its wavelength larger than the wall thickness (Couade *et al.*, 2010). Ultrafast imaging with the center frequency of 5 MHz and CPWC with three steering angles (−4°, 0°, 4°) at 6000 fps was performed to capture shear wave propagation. Axial velocities of the material points between every two consecutive compounded frames were first estimated to visualize the shear wave fronts in VMP-I, and analysis of the shear wave fronts in the spatiotemporal domain yielded a group velocity map using an in-house time-of-flight algorithm (Lee *et al.*, 2012). In both uDoppler imaging and SWI, the in-phase and quadrature (IQ) data were acquired and stored for offline analysis.

2.2.2 FSI simulation modeling

FSI simulation is useful for the prediction of blood dynamics inside the lumen and shear wave propagation on the vessel wall, thus may serve as a tool to compare with the experimental results. A 3D finite-element (FE) model of FSI simulation was established with the same geometry of VMP-I using COMSOL5.3a software (Comsol Inc. Burlington, MA, USA). The 3D model of VMP-I was first imported from SolidWorks2016 to COMSOL5.3a for modelling its geometry. To apply the same boundary conditions (BCs) as those in the uDoppler imaging and SWI experiments, the upper surface of VMP-I (figure 4(a) ②) was set to be free to move, while the other surfaces were fixed in the Cartesian coordinates.

The fluid component inside the vessel lumen was defined as 'moving mesh' whereas its meshing on the inlet and outlet was fixed (figure 4(a) ④ and ⑤). The fluid properties were set to be 1037 kg/m^3 density and 4.1 mPa*s dynamic viscosity, both of which were close to those of real human blood (Ramnarine *et al.*, 1998). According to fluid mechanics, the BMF flow could be treated as 'fully developed flow' with a laminar pattern since it fulfilled the two conditions (Cengel, 2010), being 1) that its Reynolds number ($R_e = \frac{\rho V_{avg} D}{\mu} \approx \frac{1037\ \mathrm{kg/m^3} * 10\ \mathrm{cm/s} * 10\ \mathrm{mm}}{4.1\ \mathrm{mPa \cdot s}} = 252.9$, fluid density ρ, average fluid velocity V_{avg}, entrance diameter D) was smaller than the critical value 2300, and 2) that the entrance length in the experimental setup (figure 3(d)) was larger than $L_{entr} \approx 0.05 R_e D = 0.05 * 252.9 * 10\ \mathrm{mm} = 126.5\ \mathrm{mm}$ for a flow velocity profile with the maximum at the centerline after traveling through the entrance. The inlet of the simulated vessel phantom (figure 4(a) ④) was given by a 2 ml/s 'fully developed flow' due to the entrance length in figure 3(d), and its outlet (figure 4(a) ⑤) was given a 0.75 kPa pressure as measured by the pressure meter in the experimental setup.

The solid components in the FSI model were defined as a Gent hyperelastic material to exhibit the strain stiffening effect with a nearly incompressible property (100 MPa bulk modulus) and 1000 kg/m^3 density. Uniaxial tension was conducted on the PVA-H samples with 3 F/T cycles and the PVA-H samples with 5 F/T cycles, respectively. The corresponding experimental data were then fitted with the Gent model to obtain the material parameters (shear modulus μ and nonlinearity parameter J_m). From the mechanical test results, shear modulus μ of the surrounding medium was measured to be 18.028 kPa, and that of the vessel wall was 30.101 kPa, both of which were close to the reported values (Fromageau et al., 2003). Both had J_m=2.0256, which was the material parameter in the Gent model to regulate its nonlinearity.

Note that the vessel wall was 1.67 times stiffer than the surrounding medium at no deformation in the FSI simulation. The wall condition between the fluid and the solid was defined as 'no-slip' to consider FSI accurately. Both the fluid and the solid were meshed using the free tetrahedral element with different element sizes controlled by the 'physics-induced' method in COMSOL5.3a. A predefined 'fine' element size for 'fluid dynamics' was used for the fluid component and its boundaries with the solid, while a predefined 'normal' element size for 'general physics' was used for the solid components. Moreover, the solid and fluid components were meshed with the linear element and 'P1+P1', respectively, resulting in a total of 160,868 elements as shown in figure 4(b).

Finally, the 'fully coupled' solver with its default setting was chosen to compute the FSI scenario of VMP-I for both fluid dynamics inside its vessel lumen and shear wave propagation on its vessel wall. The FSI simulation for fluid dynamics was computed in a stationary condition (i.e., constant flow). The simulated flow velocity in the *Z* direction (*w_fluid*) and that in the *X* direction (*u_fluid*) in the central *X*-*Z* plane were outputted (figure 4(b)) and compared with those estimated by uDoppler imaging.

Because the FSI simulation for shear wave propagation was time-dependent, a 1×10^8 N/m^3 body force with a profile of 100-μs Gaussian pulse was applied along the -*Z* direction in a cylindrical region of 0.5 mm radius and acted on the vessel wall to generate shear waves. The time-dependent FSI simulation was finally run within 200 sub-steps for 2 ms. Also, in the central *X*-*Z* plane (figure 4(b)), the simulated *Z* displacements (*w_solid*) of the solid components were outputted to visualize the shear wave propagation. The group velocity of the shear wave was calculated using the same time-of-flight algorithm as the one used for experimental data (see Section 2.2.1). Note that only 2

minutes 24 seconds was needed to run the stationary FSI simulation on a PC with Intel i5 processor and 32G memory, whereas the time-dependent simulation took 1 hour 25 minutes. All data analysis was done in Matlab2017b (The MathWorks, Natick, MA, USA).

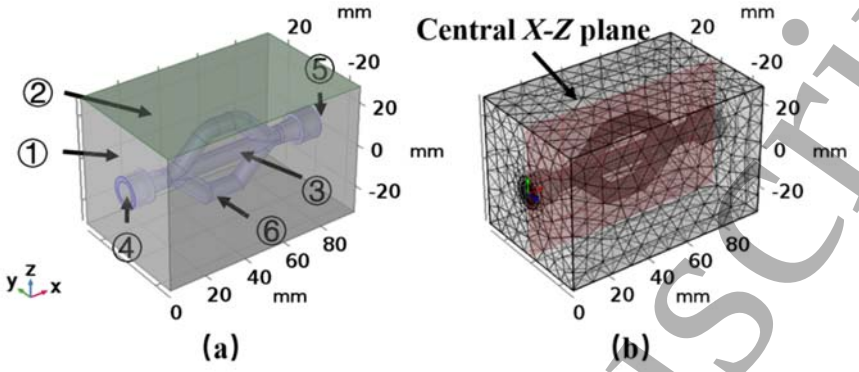

Figure 4. (a) Geometry of vessel-mimicking phantom I (VMP-I) in the FSI simulation. ① surrounding medium of VMP-I; ② free surface (shaded in green color) of the surrounding medium while other surfaces being fixed; ③ vessel lumen of VMP-I; ④ and ⑤ inlet and outlet of the blood flow inside VMP-I, respectively; ⑥ vessel wall (shaded in blue color); **(b) tetrahedral meshing of VMP-I and the central *X*-*Z* plane** (shaded in red color). Note that the fluid component was meshed with a predefined 'fine' element size for 'fluid dynamics', while the solid components were meshed with a predefined 'normal' element size for 'general physics'.

3 Results

3.1 B-mode imaging and PDI on VMPs I

The vessel lumen and wall structure of VMP-I were clearly observed in its longitudinal view from the B-mode image (figure 5(a)). This verified that the vessel core of VMP-I printed by the water-soluble PVA filament had been dissolved completely, and the lumen geometry was successfully fabricated. Measured from B-mode images of VMP-I, the inner diameter was 4.23±0.27 mm, and the wall thickness was 1.98±0.01 mm. Both were in good agreement with the ground truths (4 mm inner diameter and 2 mm thickness). The thickness of paraffin wax was estimated to be about 0.1 mm by comparing the size of inner diameter of VMP-I (4.23 mm) with the ground truth (4 mm). No irregular surfaces were noticed inside VMP-I, confirming successful fabrication of VMP-I.

The power Doppler image of VMP-I in the longitudinal view is shown in figure 5(b), where power Doppler signal of the BMF was obtained at the steering angle of $-15°$ in the region of interest (ROI), color coded using a 'hot' colormap. Figure 5(b) shows that the BMF, which was driven by the AccuFlow-Q pump (2 ml/s constant flow, 0.75 kPa outlet pressure), flowed through the lumen of VMP-I from its inlets to outlets.

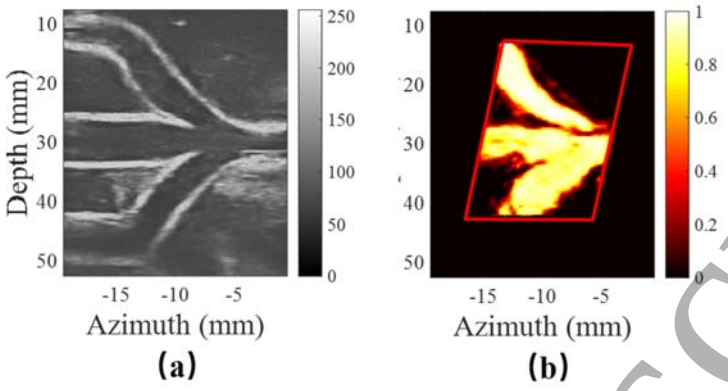

Figure 5. (a) B-mode image of vessel-mimicking phantom I (VMP-I); (b) power Doppler image of VMP-I. Red parallelogram represents the ROI for power Doppler imaging. Note that the inlet and the outlet were on the left and right sides, respectively, and the blood mimicking fluid (BMF) flowed rightwards in (b).

3.2 Experimental and simulated blood dynamics and shear wave propagation on VMP-I

To preliminarily evaluate blood dynamics in VMP-I, flow velocities inside its lumen were estimated by uDoppler imaging and compared with the values from the FSI simulation in a scenario of 2 ml/s constant flow and 0.75 kPa outlet pressure. In the top row of figure 6(a), positive axial flow velocities (V_a) indicated upward movement of the BMF for V_a and were displayed in warm color. For the lateral flow velocities (V_l) in the bottom row of figure 6(a), positive values represent rightward movement of the BMF and are coded in warm color. Cool colors indicate the opposite BMF directions for both V_a and V_l. The estimated V_a distribution in the upper-left image in figure 6(a) shows that the BMF moved upwards in the ascending part of the upper branch, while it moved downwards in the descending part of the bottom branch. The flow pattern with the maximum flow velocity in the centerline was well portrayed by V_a in these two segments. The estimated V_l map shows rightward flow of the BMF in all the three branches but with a larger speed in the middle one (figure 6(a), bottom left). Overall, the estimated V_a image was less noisy than the estimated V_l image as shown in figure 6(a); the estimated flow direction in the VMP-I was accurate except for the rightmost 10 mm segment of the bottom branch, whose V_l estimates were negative and interpreted as a leftward flow (figure 6(a), bottom left).

The estimated flow velocities were generally in good quantitative agreement with simulated ones (red rectangles in figure 6(a), right column). Figure 6(b) left column shows the absolute difference maps of V_a and V_l between the estimation and the ground truth, while their corresponding percent difference maps are shown in the right column. In the ROIs (red parallelograms in figures 6(b)), average V_a was found to be overestimated by 0.81 cm/s, which led to a 14.5% relative difference, while average V_l was underestimated by 1.15 cm/s, which was equivalent to -20.2% relative difference. V_a was not estimated accurately in the areas with a small axial flow velocity. Figure 6(c) shows vector plots of the BMF flow, and the estimated flow velocity vectors agreed with the simulated ones qualitatively, particularly in the middle branch. Moreover, a laminar flow was observed as smooth layers of the fluid to characterize the ordered fluid motion as defined in (Cengel, 2010). The parallel streamlines, which were plotted using the built-in function 'streamline' in

MATLAB, confirmed the laminar patterns for both the estimated BMF flow and the simulated one from the magnified images.

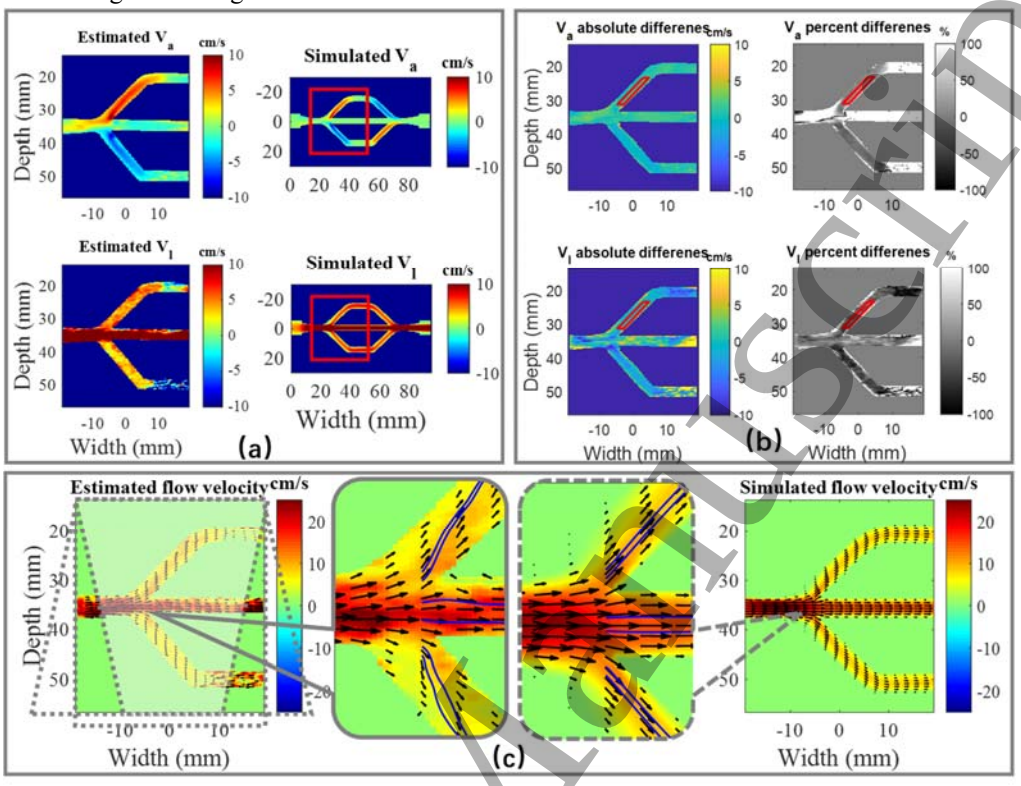

Figure 6. (a) The estimated and simulated axial and lateral flow velocities in vessel-mimicking phantom I (VMP-I) in the longitudinal view under 2 ml/s constant flow and 0.75 kPa outlet pressure (red rectangles are the ROIs for quantitative comparison); **(b) Spatial maps of absolute and percent differences of axial and lateral flow velocities in VMP-I between the estimated values by uDoppler imaging and the simulated ones from the FSI simulation** (red parallelograms represent the ROIs for mean value calculation); **(c) 2D vector plots of the estimated and simulated flow velocities** (dashed parallelograms represent the steered plane waves with their overlapping region as shown in gray color for uDoppler imaging; blue lines in the magnified views represent the streamlines of the BMF flow).

The left column of figure 7(a) show propagation of shear waves in the walls of the three branches of VMP-I at 0.5 ms, 1 ms and 1.5 ms after their generation, where the wave fronts of shear waves were identified by the red arrows. Figure 7(a) right shows the estimated shear wave speed map, where the warm color indicates a positive speed value for the rightward shear wave. The average estimated group velocity in all the regions through which shear wave propagated was 5.1 m/s (Figure 7(a), right). Figure 7(b) shows the simulated shear wave propagation in the three branches of VMP-I at 1 ms in a 3D view of the FSI simulation, from which the *Z* displacement values (i.e., axial displacement values in the ultrasound imaging coordinates) of the central *X*-*Z* plane was exported and displayed as the longitudinal view of VMP-I. From the spatiotemporal map of the shear wave at the depth of interest, the simulated group velocity was calculated to be 5.4 m/s, which was in good agreement with the estimated one.

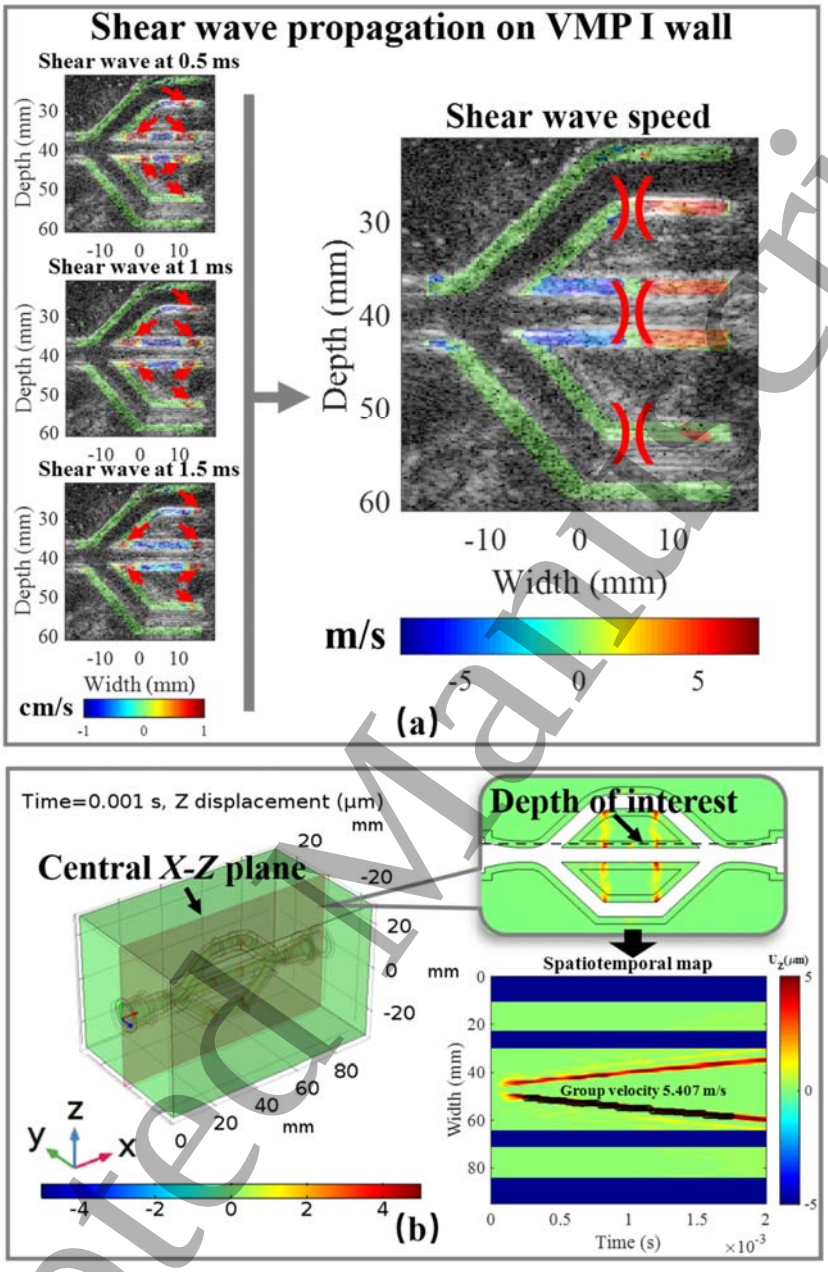

Figure 7. (a) Shear wave propagation and its group velocity map for the walls of vessel-mimicking phantom I (VMP-I) using shear wave imaging (SWI) (left column: the wave fronts of shear waves at multiple time points (0.5 ms, 1 ms, 1.5 ms) are identified by red arrows; right: negative speed indicates the leftward shear wave, and positive speed represents the rightward shear wave, the foci are marked by red curves); **(b) The simulated shear wave propagation on vessel walls of VMP-I in a 3D view; axial displacements (U_Z) in the central *X*-*Z* plane** (shaded in red color) are the shear wave amplitudes and mapped. **A group velocity was then calculated from the spatiotemporal map at the depth of interest**.

4 Discussion

In this paper, a method was explored to fabricate walled VMPs for ultrasound imaging using FDM 3D printing with a water-soluble PVA filament. The capability of our proposed method was tested for fabricating walled VMPs, instead of wall-less ones. Therefore, our work was different from a study published very recently (Mackle et al., 2019). Unaware of the study by Mackle et al., we developed our fabrication method separately in 2017 and have been optimizing the protocol. In particular, as a key to the final success, paraffin wax was used to isolate the PVA-printed vessel core and PVA-H during fabrication. The advantages of paraffin wax, including coating with ease (i.e., without any special equipment), satisfactory thickness (~0.1 mm), chemical stability, easy removal after fabrication, make the proposed method more practicable for ultrasound imaging studies. A walled three-branch VMP (VMP-I) was made for illustration. The dissolution of PVA-printed vessel core of VMP-I was first substantiated by B-mode imaging and PDI, confirming fabrication of VMP-I with good geometric accuracy (figure 5). Because VMP-I could be used in ultrasound flow imaging and ultrasound elastography, it was tested by uDoppler imaging and SWI to respectively estimate its flow velocities inside the lumen and shear wave speeds of the vessel wall. Results showed good agreement between ultrasound estimations and the FSI simulation, demonstrating that the proposed fabrication method was feasible to make walled VMPs safely, efficiently and flexibly. The walled VMPs were useful to serve as the ground truths for ultrasound flow imaging and ultrasound elastography. Together with the FSI simulation, a walled VMP is deemed as a useful tool for a better understanding of blood dynamics and wall stiffness of the blood vessel and for the development of ultrasound imaging techniques.

The proposed fabrication method for the VMPs has three key steps: the vessel core preparation, the VMP fabrication, and the vessel core dissolution (figure 1). Different from the conventional use of the water-soluble PVA filament as a supporting material, it is used herein to print the vessel core directly to tackle the issues of solvent toxicity and dissolution time reported in literature. During fabrication, the humidity should be carefully controlled; otherwise, the water-soluble PVA filament might be dampened and become too soft to print well. In this study, both a filament dryer and a dehumidifier were used in a closed room while printing. The humidity in the closed room could be controlled below 40% to guarantee good printing quality of the vessel core. In addition, the printed vessel core might be dissolved by the water content in the PVA-H solution, so a layer of paraffin wax, which does not chemically react with the water-soluble PVA filament or the PVA-H solution, was applied here to insulate the two during fabrication. Paraffin wax melts to the liquid state when heated upon its melting point (56℃) and quickly goes back to a solid state under the room temperature. By dipping the vessel core into the melted paraffin wax, a uniform layer of paraffin wax can be made to cover the entire vessel core, making it a convenient insulator. As confirmed on VMP-I, without using any special equipment, the thickness of the paraffin wax (0.1 mm) was about 5% to the diameter of the vessel core, which was acceptable for fabrication. Although a thinner insolation layer (~3 μm, parylene) could be achieved as reported (Mackle et al., 2019), the need of special equipment for coating parylene hinders its widespread use. In this study, prior to the filling of the PVA-H solution, which should freeze quickly to ensure the homogeneity of the final VMP, the vessel core with its casting box had been placed into a -20℃ freezer for 1 hour to lower the temperature.

In our experience, the inhomogeneity of the PVA-H phantom, which is more exacerbated in large phantoms, is caused by the precipitation of ultrasound scatterers due to the slow freezing

process in the first F/T cycle. Increasing the freezing rate might reduce the precipitation of ultrasound scatterers and the inhomogeneity of the PVA-H phantom, so all the boxes were stored in the freezer in advance to accelerate the freezing procedure of PVA-H. The inhomogeneity issue may be resolved by using other tissue-mimicking materials (McLeod et al., 2016; McLeod et al., 2015; Culjat et al., 2010; Maneas et al., 2018), instead of PVA-H, with the proposed method. As proposed in an earlier study, the vessel core could be printed by a PLA filament with good printing quality, but it had to be dissolved by Chloroform (Ho *et al.*, 2017), which is a toxic solution and must be handled in a fume cupboard for safety, thus limiting its application. An HIPS (High Impact Polystyrene) filament is commonly used as a supporting material in FDM 3D printing, for it can be dissolved in Limonene; however, it becomes too sticky to remove after its time-consuming dissolution, especially for the VMP fabrication in this study. For example, the dissolution time of the vessel core made of the water-soluble PVA filament was 3 hours, whereas that of the HIPS-based ones took more than 24 hours in our preliminary tests.

B-mode imaging was performed to visualize the interior of VMP-I (figures 5(a)) and measure its geometric parameters. While overall VMP-I was of high quality, the vessel core was not printed perfectly with 4 mm diameter because of the intrinsic printing error caused by the 0.4 mm nozzles and the finite spatial resolutions in different directions (see Section 2.1.1). An FDM 3D printer with higher spatial resolution is recommended for the proposed method if available. The applied layer of paraffin wax might not be too thin to be negligible for small-sized vessel core (< 2 mm diameter). There might be some human errors during manual size measurement. Despite the aforementioned sources of errors, good geometric accuracy of fabricated VMP-I was still demonstrated by comparing to the ground truth. From the power Doppler image in figure 5(b), the Doppler signals generated by the moving BMF indicated the BMF flowing inside the vessel lumens of VMP-I from the inlet of the pumping box to the outlet. The information from B-mode imaging and PDI together confirmed that the PVA-printed vessel core of VMP-I was dissolved completely. Potentially, VMPs with small vessel lumens (~2 mm diameter, ~10% geometric error) can be made by the proposed method and used in PDI experiments for investigating the blood flow in small vessels.

The fluid velocity and shear wave propagation in VMP-I were examined by uDoppler imaging and SWI, respectively, and verified in FSI simulations. V_a was overestimated by 14.5%, while V_l was underestimated by 5.2% with respect to the simulated flow velocities in the ROIs (red parallelograms in figure 6(b)), resulting in 0.8% underestimation of the magnitude of the flow velocity. One might note that relatively good estimation of both V_a and V_l occurred in the regions with small Doppler angles under appropriate flow velocities, for instance, the average Doppler angle was 30º, $V_a \geq 5.02$ cm/s and $V_l \geq 2.59$ cm/s in the ROI in figure 6(b).The horizontal segments of all the three branches for V_a and the boundaries between vessel walls and BMF had an overestimation of V_a and V_l. The FSI simulation results in the right panel of figure 6 (c) showed the flow velocity distribution and vectors in the ideal scenario, where the flow pattern was laminar and exhibited smooth and layered BMF flow as manifested by the parallel streamlines in each branch of VMP-I. Moreover, the BMF should be developed fully to have a flow velocity profile with the maximum in the centerline of the lumen in such ideal case. In contrast, , the experimental BMF flow estimated by uDoppler imaging in the left panel of figure 6(c) did not exhibit fully developed flow but could be considered as a laminar flow as identified by the quasi-parallel streamlines in each branch of VMP-I. Comparing the estimated flow velocity with the simulated one in each row of figure 6(a), Va was better estimated than Vl in terms of the flow velocity profile with the maximum

in the centerline. Poorer estimation of V_l than V_a in ultrasound Doppler imaging owing to the inherently low sampling rate and lack of phase information in the lateral direction in ultrasound imaging. Further efforts for better flow velocity estimation accuracy should be focused on the V_l component. There were two possible sources of differences from the experimental setup (figure 3(d)). One was the small leakage of BMF that was found at the inlet and outlet of VMP-I during the experiments although tie bands were used to reduce the leakage. The other was that the imaging plane in uDoppler imaging and the central *X-Z* plane in the FSI simulation might not have been perfectly matched. Several factors may have affected the accuracy of flow velocity estimation by uDoppler imaging, such as the Doppler angles, the imaging depth, the velocity magnitude, the number and range of steering angles, and compounded frame rates (Bercoff *et al.*, 2011). The influence of these factors on flow velocity estimation in uDoppler imaging should be an area for systematic investigations, where VMP-I can serve as a useful tool for that.

For shear wave propagation on the vessel walls of VMP-I, group velocity, instead of phase velocity from the dispersion analysis, was calculated for an illustration purpose in both SWI and the FSI simulation. One might observe that the shear wave at the bottommost branch was not effectively generated due to the attenuated acoustic radiation force (ARF) through layers of the BMF in the vessel lumen and the surrounding bulk medium. The average estimated group velocity was 5.1±1.5 m/s by SWI and agreed well with the simulated one (=5.4 m/s), resulting in -6.03% difference. Note that both the estimated group velocity and the calculated one in the simulation were slightly smaller than the theoretical value, (= 5.5 m/s for the vessel wall with 30.101 kPa μ based on $\rho v^2 = \mu$, where ρ, v and μ are the density, shear wave group velocity and shear modulus, respectively). The group velocity of the shear wave might be influenced by the interaction among the vessel wall, the surrounding medium and BMF inside the vessel lumens of VMP-I for the experimental setup used in SWI (figure 3(d)) (Lee *et al.*, 2018). This phenomenon corroborated the necessary incorporation of FSI into the analysis of shear wave propagation on vessel walls. The small discrepancy between SWI and the FSI simulation might result from two factors. One was that the FSI simulation treated VMP as a purely elastic material without considering the viscosity of PVA-H. The other was that the real stiffnesses of the vessel wall and the surrounding medium of VMP-I might be slightly different from those used in the FSI simulation (Fromageau *et al.*, 2003).

The proposed method can be also utilized to fabricate a wall-less VMP with a vessel lumen of complex geometry (figure 1). For illustration, a wall-less VMP (VMP-II) was made by following the steps in figure 1. Its geometry (4 mm diameter) was referenced to a simplified coronary artery model scaled by 0.5. Figures 8(a) shows the 3D model for the vessel core of VMP-II, and figure 8(b) shows the PVA-printed vessel core of VMP-II in the holding box before pouring in the PVA-H solution (10% PVA-H powders, 1% SiO_2, 1% potassium sorbate, DI water). After fabrication, VMP-II was examined by B-mode imaging and PDI using the same experimental setup for VMP-I. The B-mode image of VMP-II confirmed that it was fabricated with good geometrical accuracy (figure 8(c)), and the power Doppler image of VMP-II confirmed that its PVA-printed vessel core was fully dissolved (figure 8(d)). This VMP-II demonstrated the feasibility of the proposed method for fabricating a vessel lumen of complex geometry. Because of the known ground truth of the VMP-II geometry, it could serve as a good tool for testing and improving the quality of 2D and 3D functional ultrasound imaging techniques for blood vessels.

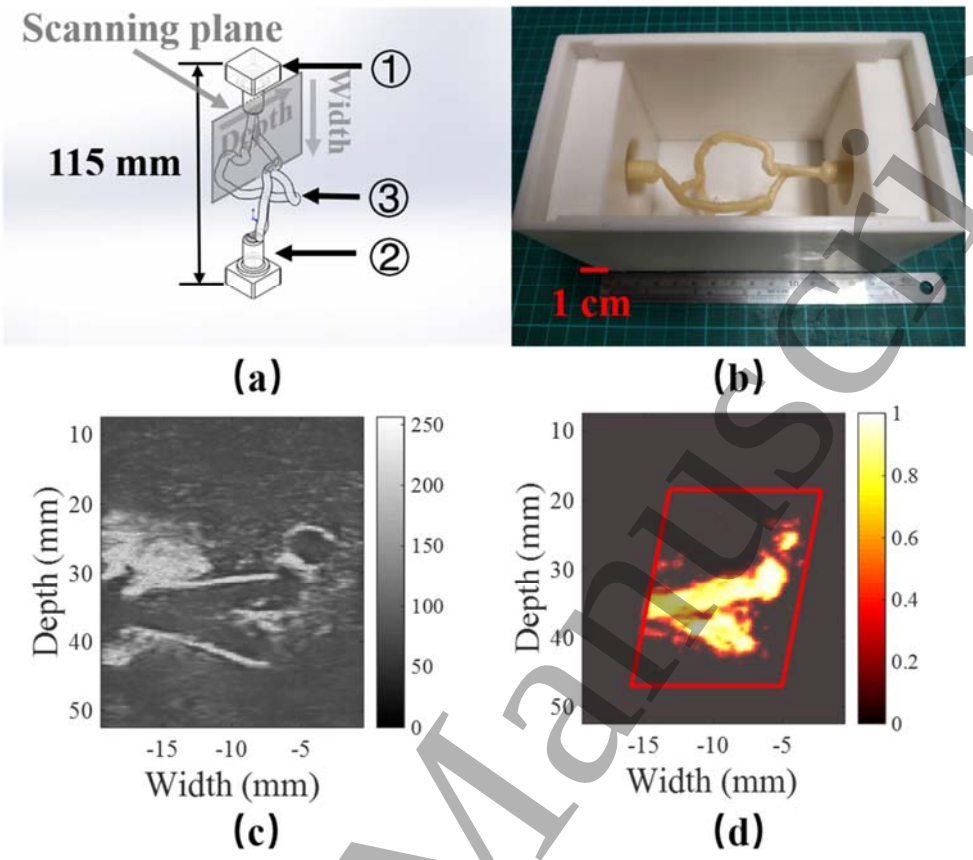

Figure 8. (a) 3D model of the vessel core for vessel-mimicking phantom II (VMP-II) and the scanning plane for B-mode imaging and PDI, ① the holding part, ② the connecting part and ③ the major vessel structure (4 mm in diameter); **(b) The vessel core of VMP-II (water-soluble PVA, wall-less) in the holding box (PLA)**. Note that all the models in (b) were printed by CreatBot DX plus; **(c) and (d) B-mode image and power Doppler image of VMP-II in the scanning plane, respectively.**

The proposed method may ultimately have a potential application in patient-specific interventions or therapies, where VMPs with lumen geometries that are designed based on real patient data from MRI or CT images can be fabricated for studying unique problems of blood flow and offering a tailor-made treatment plan for each patient. Using the proposed method, various customized VMPs, such as vasculature of different organs, can be fabricated given particular research purposes. It is also feasible to fabricate VMPs for other medical imaging modalities, such as MRI.

5 Conclusion

This paper presents a method that utilizes an FDM 3D printing technique and a water-soluble PVA filament with paraffin wax as the isolator to fabricate walled VMPs safely, efficiently, and flexibly. By directly printing the vessel core using the water-soluble PVA filament and dissolving it in water at the final stage of fabrication, the proposed method avoids the use of toxic solvents and long dissolution time. A three-branch walled VMP (VMP-I) was fabricated to exemplify vessel wall structure. B-mode imaging and PDI were used to visualize the lumen of VMP-I to confirm its good

fabrication quality. VMP-I was further examined by uDoppler imaging, SWI, and FSI simulation for the flow conditions in vessel lumens and the wall stiffness. Together with the FSI simulation, the proposed fabrication method is envisioned to serve as an essential experimental tool to innovate, evaluate, and optimize ultrasound imaging techniques for blood vessels.

Acknowledgment

This study was supported by National Natural Science Foundation of China (NSFC)/Research Grants Council (RGC) Joint Research Scheme (N_HKU713_15).

References

Bercoff J, Montaldo G, Loupas T, Savery D, Mézière F, Fink M and Tanter M 2011 Ultrafast compound Doppler imaging: Providing full blood flow characterization *IEEE Transactions on Ultrasonics, Ferroelectrics and Frequency Control* **58** 134-47

Bercoff J, Tanter M and Fink M 2004 Supersonic shear imaging: a new technique for soft tissue elasticity mapping *IEEE transactions on ultrasonics, ferroelectrics, and frequency control* **51** 396-409

Cengel Y A 2010 *Fluid mechanics*: Tata McGraw-Hill Education)

Chatelin S, Bernal M, Deffieux T, Papadacci C, Flaud P, Nahas A, Boccara C, Gennisson J-L, Tanter M and Pernot M 2014 Anisotropic polyvinyl alcohol hydrogel phantom for shear wave elastography in fibrous biological soft tissue: a multimodality characterization *Physics in medicine and biology* **59** 6923

Chee A J, Ho C K, Yiu B Y and Yu A C 2016 Walled carotid bifurcation phantoms for imaging investigations of vessel wall motion and blood flow dynamics *IEEE Trans. Ultrason., Ferroelect., Freq. Control* **63** 1852-64

Couade M, Pernot M, Prada C, Messas E, Emmerich J, Bruneval P, Criton A, Fink M and Tanter M 2010 Quantitative assessment of arterial wall biomechanical properties using shear wave imaging *Ultrasound in medicine & biology* **36** 1662-76

Cournane S, Fagan A and Browne J 2012 Review of ultrasound elastography quality control and training test phantoms *Ultrasound* **20** 16-23

Culjat M O, Goldenberg D, Tewari P and Singh R S 2010 A review of tissue substitutes for ultrasound imaging *Ultrasound in medicine & biology* **36** 861-73

Demené C, Deffieux T, Pernot M, Osmanski B-F, Biran V, Gennisson J-L, Sieu L-A, Bergel A, Franqui S and Correas J-M 2015 Spatiotemporal clutter filtering of ultrafast ultrasound data highly increases Doppler and fUltrasound sensitivity *IEEE transactions on medical imaging* **34** 2271-85

Evans D H, Jensen J A and Nielsen M B 2011 Ultrasonic colour Doppler imaging *Interface focus* **1** 490-502

Fromageau J, Brusseau E, Vray D, Gimenez G and Delachartre P 2003 Characterization of PVA cryogel for intravascular ultrasound elasticity imaging *IEEE transactions on ultrasonics, ferroelectrics, and frequency control* **50** 1318-24

Fromageau J, Gennisson J-L, Schmitt C, Maurice R L, Mongrain R and Cloutier G 2007 Estimation of polyvinyl alcohol cryogel mechanical properties with four ultrasound elastography methods and comparison with gold standard testings *IEEE transactions on ultrasonics, ferroelectrics, and frequency control* **54**

Guo Y, Lo H Y and Lee W-N 2017 Transmural transverse stiffness estimation in vascular shear wave imaging: A simulation and phantom study *Applied Physics Letters* **110** 193701

Guo Y, Wang Y, Chang E J-H and Lee W-N 2018 Multidirectional estimation of arterial stiffness using vascular guided wave imaging with geometry correction *Ultrasound in medicine & biology* **44** 884-96

He Q, Li G-Y, Lee F-F, Zhang Q, Cao Y and Luo J 2017 Novel method for vessel cross-sectional shear wave imaging *Ultrasound in medicine & biology* **43** 1520-32

Ho C K, Chee A J, Yiu B Y, Tsang A C, Chow K W and Alfred C 2017 Wall-less flow phantoms with tortuous vascular geometries: Design principles and a patient-specific model fabrication example *IEEE transactions on ultrasonics, ferroelectrics, and frequency control* **64** 25-38

Hoskins P R 2007 Physical properties of tissues relevant to arterial ultrasound imaging and blood velocity measurement *Ultrasound in medicine & biology* **33** 1527-39

Hudson-Dixon C M, Long B W and Cox L A 1999 Power Doppler imaging: principles and applications *Radiologic technology* **70** 235-

Lai S S, Yiu B Y, Poon A K and Alfred C 2013 Design of anthropomorphic flow phantoms based on rapid prototyping of compliant vessel geometries *Ultrasound in medicine & biology* **39** 1654-64

Lee W-N, Chang E J-H, Guo Y and Wang Y 2018 Experimental investigation of guided wave imaging in thin soft media under various coupling conditions *Ultrasound in medicine & biology* **44** 2821-37

Lee W-N, Pernot M, Couade M, Messas E, Bruneval P, Bel A, Hagege A A, Fink M and Tanter M 2012 Mapping myocardial fiber orientation using echocardiography-based shear wave imaging *IEEE transactions on medical imaging* **31** 554-62

Luyet C, Hartwich V, Urwyler N, Schumacher P, Eichenberger U and Vogt A 2011 Evaluation of a novel needle guide for ultrasound-guided phantom vessel cannulation *Anaesthesia* **66** 715-20

Mackle E C, Maneas E, Little C, Carr E, Xia W, Nikitichev D, Rakhit R D, Finlay M C and Desjardins A E *Design and Quality for Biomedical Technologies XII,2019),* vol. Series 10870*)*: International Society for Optics and Photonics) p 108700P

Maneas E, Xia W, Nikitichev D I, Daher B, Manimaran M, Wong R Y J, Chang C-W, Rahmani B, Capelli C and Schievano S 2018 Anatomically realistic ultrasound phantoms using gel wax with 3D printed moulds *Physics in Medicine & Biology* **63** 015033

Maurice R L, Daronat M, Ohayon J, Stoyanova E, Foster F S and Cloutier G 2005 Non-invasive high-frequency vascular ultrasound elastography *Physics in Medicine & Biology* **50** 1611

McLeod A J, Baxter J S, Ameri G, Ganapathy S, Peters T M and Chen E C 2015 Detection and visualization of dural pulsation for spine needle interventions *International journal of computer assisted radiology and surgery* **10** 947-58

McLeod A J, Currie M E, Moore J T, Bainbridge D, Kiaii B B, Chu M W and Peters T M 2016 Phantom study of an ultrasound guidance system for transcatheter aortic valve implantation *Computerized Medical Imaging and Graphics* **50** 24-30

Millon L, Mohammadi H and Wan W 2006 Anisotropic polyvinyl alcohol hydrogel for cardiovascular applications *Journal of Biomedical Materials Research Part B: Applied Biomaterials* **79** 305-11

Pavan T Z, Madsen E L, Frank G R, Carneiro A A O and Hall T J 2010 Nonlinear elastic behavior of phantom materials for elastography *Physics in Medicine & Biology* **55** 2679

Ramnarine K V, Nassiri D K, Hoskins P R and Lubbers J 1998 Validation of a new blood-mimicking fluid for use in Doppler flow test objects *Ultrasound in medicine & biology* **24** 451-9

Ryan L K and Foster F S 1997 Tissue equivalent vessel phantoms for intravascular ultrasound *Ultrasound in medicine & biology* **23** 261-73

Shahmirzadi D, Li R X and Konofagou E E 2012 Pulse-wave propagation in straight-geometry vessels for stiffness estimation: theory, simulations, phantoms and in vitro findings *Journal of biomechanical engineering* **134** 114502

Surry K, Austin H, Fenster A and Peters T 2004 Poly (vinyl alcohol) cryogel phantoms for use in ultrasound and MR imaging *Physics in Medicine & Biology* **49** 5529

Tanter M and Fink M 2014 Ultrafast imaging in biomedical ultrasound *IEEE transactions on ultrasonics, ferroelectrics, and frequency control* **61** 102-19

Vappou J, Luo J and Konofagou E E 2010 Pulse wave imaging for noninvasive and quantitative measurement of arterial stiffness in vivo *American journal of hypertension* **23** 393-8

Wang Y, Li H, Guo Y and Lee W-N 2019 Bidirectional Ultrasound Elastographic Imaging Framework for Non-invasive Assessment of the Non-linear Behavior of a Physiologically Pressurized Artery *Ultrasound in medicine & biology*

Wei L, Williams R, Loupas T and Burns P N *2018 IEEE International Ultrasonics Symposium (IUS),2018),* vol. Series*)*: IEEE) pp 1-9

White D, Duck F, Fairhead A, Rothenberg L, Shaw A, Zagzebski J and Zankl M 1998 Tissue substitutes, phantoms and computational modelling in medical ultrasound *ICRU Report*

WHO 2017 https://www.who.int/en/news-room/fact-sheets/detail/cardiovascular-diseases-(cvds).

Wong E Y, Thorne M L, Nikolov H N, Poepping T L and Holdsworth D W 2008 Doppler ultrasound compatible plastic material for use in rigid flow models *Ultrasound in medicine & biology* **34** 1846-56

Xia W, Piras D, Heijblom M, Steenbergen W, Van Leeuwen T G and Manohar S 2011 Poly (vinyl alcohol) gels as photoacoustic breast phantoms revisited *Journal of biomedical optics* **16** 075002

Yiu B Y and Alfred C 2013 High-frame-rate ultrasound color-encoded speckle imaging of complex flow dynamics *Ultrasound in medicine & biology* **39** 1015-25

Yiu B Y, Chee A J, Tang G, Luo W and Yu A C 2019 High frame rate doppler ultrasound bandwidth imaging for flow instability mapping *Medical physics*

Yiu B Y, Lai S S and Alfred C 2014 Vector projectile imaging: Time-resolved dynamic visualization of complex flow patterns *Ultrasound in medicine & biology* **40** 2295-309